A. Cloutier et al. (2009) model adaptations

The Cloutier et al. (2009) model reduces the full Krebs cycle into a single equation aimed at capturing the production of ATP from pyruvate (PYR), dependent on adenosine diphosphate (ADP) and oxygen (O_2) concentrations, with Michaelis-Menten kinetics as

$$v^i_{mito} = v^i_{max,mito}\left[\frac{[PYR]_i}{[PYR]_i+K_{m,PYR}}\right]\left[\frac{[ADP]_i}{[ADP]_i+K_{m,ADP}}\right]\left[\frac{[O_2]_i}{[O_2]_i+K_{m,O_2}}\right], \quad \text{(A1)}$$

where i stands for the astrocyte or the neuron, $v^i_{max,mito}$ is the maximum rate of ATP production and $K_{m,PYR}$, $K_{m,ADP}$, $K_{m,O2}$ are the Michaelis-Menten rates for PYR, ADP and O2 respectively.

This assumption for the representation of the metabolic rate has been taken in many models in the field of neurological metabolism aimed at studying neural stimulation starting with the work by Aubert and Costalat (2002). However, as the NMO model is aimed at stimulating a stress scenario, further refinement is required here. Following Cloutier et al. (2009) Eq. 11 was extended with the bidirectional reaction (reduction/oxidation) of nicotinamide adenine dinucleotide (NAD) between NAD^+ and NADH. NAD and NADH were also assumed to reduce/oxidize with Michaelis-Menten kinetics. The new Krebs cycle equation ($v^i_{mito,new}$) is then defined as:

$$v^i_{mito,new} = v^i_{mito}\left[\frac{[NAD]_i}{[NAD]_i + K_{m,NAD}}\right]\left[\frac{[NADH]_i}{[NADH]_i + K_{m,NADH}}\right] \quad \text{(A2)}$$

where $K_{m,NAD}$ and $K_{m,NADH}$ are the Michaelis Menten parameters for NAD and NADH respectively.

Similarly, it was found that the family of models that the Cloutier et al. (2009) work is part of assumes that the metabolic reactions of hexokinase (v^i_{hk}) and phosphofructokinase (v^i_{pfk}) have a linear relationship with $[ATP_i]$. This assumption was found to result in the inability of the model to converge when simulating metabolic stress during ischaemic stroke. Therefore, to overcome this limitation, as in the case of v^i_{mito}, these rates were assumed to have a Michaelis-Menten relationship with $[ATP]$ as:

$$v^i_{hk,new} = k^i_{HK}\left[\frac{[ATP]_i}{[ATP]_i + K_{mHK,ATP}}\right]\left[\frac{[GLC]_i}{[GLC]_i + K_{m,GLC}}\right]\left[\frac{1}{1+e^{-20(G6P_n-0.6)}}\right] \quad \text{(A3)}$$

$$v^i_{pfk,new} = k^i_{PFK}\left[\frac{[ATP]_i}{[ATP]_i + K_{mPFK,ATP}}\right]\left[1+\left(\frac{[ATP]_i}{K_{I,ATP}}\right)^{nH}\right]^{-1}\left[\frac{[F6P]_i}{[F6P]_i + K_{m,F6P}}\right] \quad \text{(A4)}$$

where k^i_{HK} and k^i_{PFK} are the reaction rate constants, $[GLC]_i$, $[F6P]_i$ and $[F6P]_i$ are glucose, fructose-6-p and glucose-6-p respectively, $K_{mHK,ATP}$ and $K_{m,GLC}$ are the HK Michaelis-Menten affinity constants $K_{m,F6P}$ and $K_{mPFK,ATP}$ are the PFK Michaelis-Menten affinity constants for fructose-6-p and ATP respectively and $K_{I,ATP}$ and nH are the Hill constants for ATP.

To ensure that the behaviour of the initial model is only minimally changed by the modification, the Cloutier et al. (2009) model was refitted. The Cloutier et al. (2009) aims at capturing neuronal and glial metabolism during brain stimulation. The data used to validate

the model consists of measurements of glucose and lactate in the ECS during brain stimulation. To same measurements were used for the refit. As in Cloutier et al. (2009) the simplex method from the SBML package by Schmidt and Jirstrand (2006) was used for fitting. The fit was found to be satisfactory and is shown in Fig. A1. The values of the parameters determined by the analysis are provided Table A1.

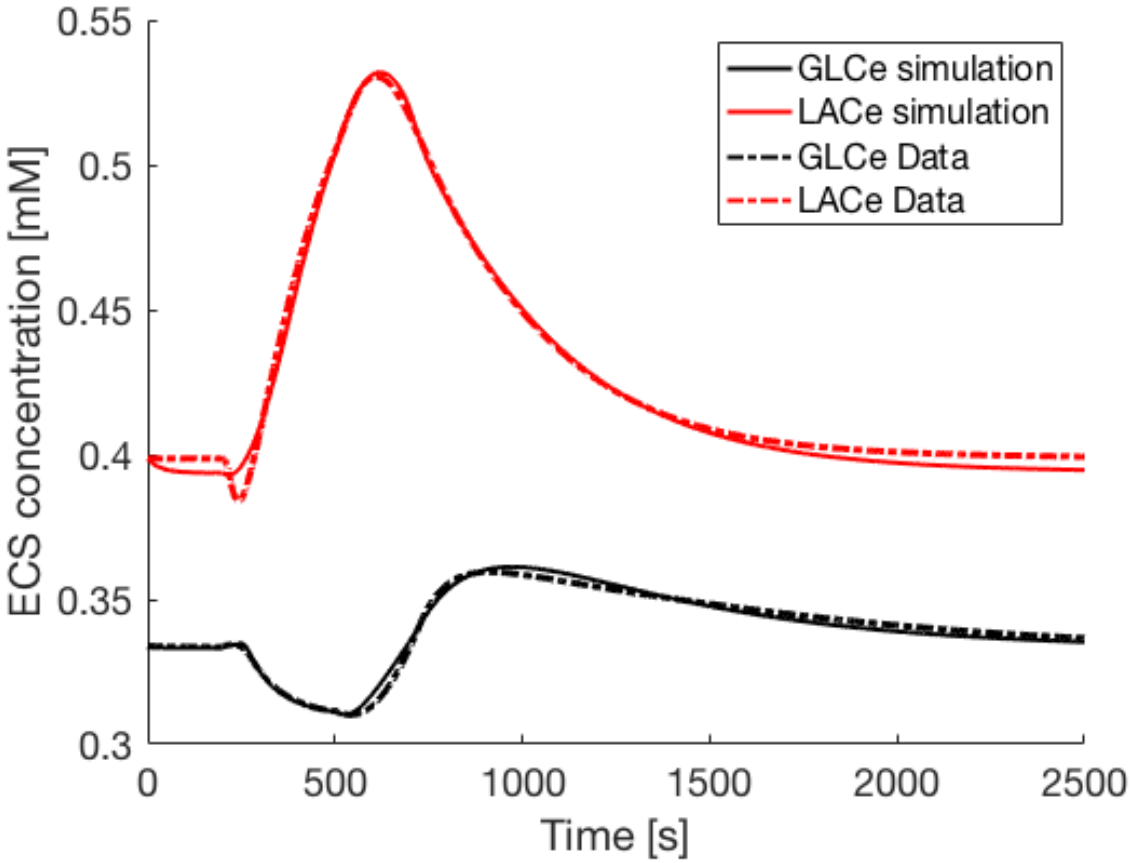

Figure A1: Revalidation of the metabolic model by Cloutier et al. (2009) after the changes presented. The data consists of lactate and glucose in the ECS measurements during brain stimulation by an action potential. The models simulation of ECS glucose and lactate concentration during action potential stimulation as in Cloutier et al. (2009) is here presented.

The solution found was stress tested by applying the Campolongo-Morris method (Saltelli *et al*. (2004)) as described in Section 3.5 in the manuscript. The test aims at evaluating how sensitive the fitting of the model is to individual changes to parameters. For this test, each parameter was varied by $\pm$5% of the fitted value. The elementary-effect (EE) for each iteration was calculated to be the difference in RMS error between every simulation and the solution presented in Figure A1. From this analysis, it was found that the parameters fall into three categories: Figure. A2I - those that perturb the RMS of the model by less than 10 percentage points (30 parameters) - Figure. A2II - those that have an absolute mean EE between 10 and 100 percentage points (15 parameters) and - Figure. A2III - the parameters that have an EE with an absolute mean larger than 100 percentage points (20 parameters).

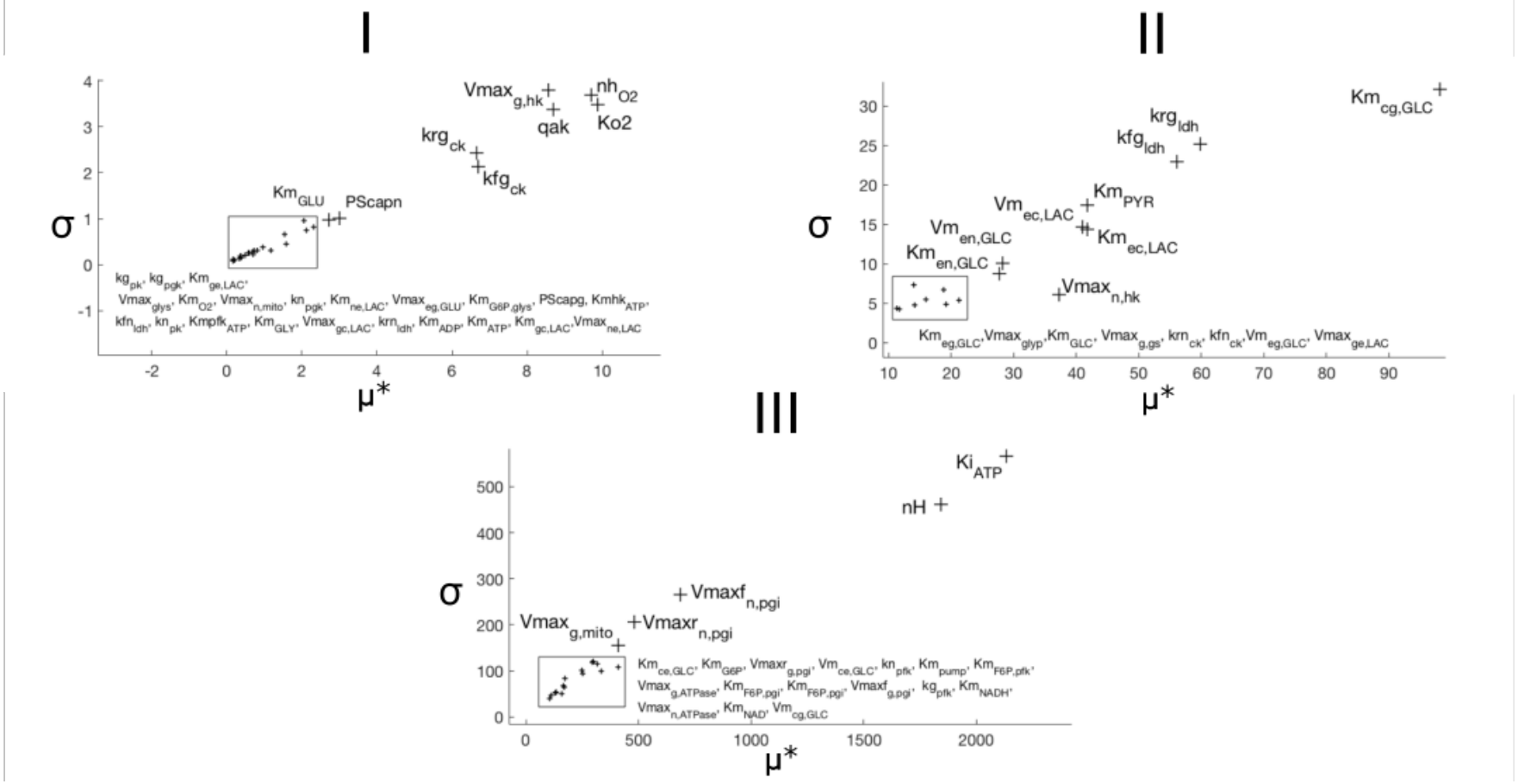

Figure A2: Results of applying the Campolongo-Morris method to the results presented in Figure A1. The EE for each iteration consisted in how varying the parameters by ±5% affect the RMS error of the fit. The distribution was found to be large and therefore the parameters were separated into three groups: I. EE's smaller than 10 percentage points, II. EE's between 10 and 100 percentage points and III. EE's above 100% percentage points.

Table A1: Refitting the parameters from Cloutier et al. (2009) **model with the new kinetics.**

Parameter	Value	Units	Description
$K_{m,en,GLC}$	14.6	mM	Affinity constant for GLC uptake by the neuron from the ECS
$V_{m,en,GLC}$	1.406	mM/s	Maximum uptake rate of GLC in astrocytes
$V_{max,n,hk}$	1.520×10^{-1}	mM/s	Maximum reaction for HK in the neuron
$V_{\mathrm{maxf,n,pgi}}$	4.775×10^{-1}	mM/s	Maximum forward reaction rate for PGI in neurons
$V_{maxr,n,pgi}$	4.451×10^{-1}	mM/s	Maximum reverse reaction rate for PGI in neurons
$K_{n,\mathrm{pfk}}$	7.219×10^{-1}	$mM^{-1}s^{-1}$	Reaction rate constant for PFK in the neuron
$K_{n,pgk}$	4.920×10^{-1}	$mM^{-1}s^{-1}$	Reaction rate constant for PGK in the neuron
$K_{\mathrm{n,pk}}$	32.779	$mM^{-1}s^{-1}$	Reaction rate constant for PK in the neuron
$K_{\mathrm{fn,ldh}}$	1.211×10^{-3}	$mM^{-1}s^{-1}$	Forward reaction rate constant for LDH in the neuron
$K_{\mathrm{rn,ldh}}$	1.819×10^{-5}	$mM^{-1}s^{-1}$	Reverse reaction rate constant for LDH in the neuron
$V_{\mathrm{max,n,mito}}$	9.171×10^{-1}	mM/s	Maximum reaction rate for the mitochondrial response for the neuron
$K_{\mathrm{m,NADH}}$	9.117×10^{-3}	mM	Affinity constant of mitochondria for NADH
$K_{\mathrm{m,NAD}}$	2.667×10^{-2}	mM	Affinity constant of mitochondria for NAD
$V_{max,ne,LAC}$	4.323×10^{-2}	mM/s	Maximum reaction rate for LAC exchange between ECS and neurons
$K_{\mathrm{m,ne,LAC}}$	3.260×10^{-6}	mM	Affinity constant for LAC exchange between ECS and neurons
$V_{\mathrm{max,n,ATPase}}$	5.289×10^{-2}	mM/s	Maximum rate of ATP consumption for cellular processes in the neuron
$K_{\mathrm{rn,ck}}$	1.344×10^{-2}	$mM^{-1}s^{-1}$	Reverse reaction rate constant for CK in the neuron
$K_{\mathrm{fn,ck}}$	4.989×10^{-2}	$mM^{-1}s^{-1}$	Forward reaction rate constant for CK in the neuron
nh_{O2}	1.3179	dimensionless	O^2 reaction order constant
PScap_n	1.793	s^{-1}	O^2 mass transfer constant between capillary and neurons
$K_{\mathrm{m,eg,GLC}}$	3.097	mM	Affinity constant for GLC exchange between ECS and astrocytes
$V_{\mathrm{m,eg,GLC}}$	2.17×10^{-2}	mM/s	Maximum rate of ATP consumption for cellular processes in the neuron
$K_{\mathrm{m,cg,GLC}}$	10.626	mM	Affinity constant for GLC exchange between capillary and astrocytes
$V_{\mathrm{m,cg,GLC}}$	8.435×10^{-3}	mM/s	Maximum rate of GLC exchange between capillaries and astrocytes

$V_{\mathbf{max,g,hk}}$	1.06×10^{-1}	mM/s	Maximum reaction rate for HK in the astrocyte
$V_{\mathbf{maxf,g,pgi}}$	4.764×10^{-1}	mM/s	Forward reaction rate for PGI in the neuron
$V_{\mathbf{maxr,g,pgi}}$	4.464×10^{-1}	mM/s	Reverse reaction rate for PGI in the neuron
$K_{\mathbf{g,pfk}}$	3.665×10^{-1}	$mM^{-1}s^{-1}$	Reaction rate constant for PFK in the astrocyte
$K_{\mathbf{g,pgk}}$	2.154×10^{-1}	$mM^{-1}s^{-1}$	Reaction rate constant for PGK in the astrocyte
$K_{\mathbf{g,pk}}$	2.335	$mM^{-1}s^{-1}$	Reaction rate constant for PK in the astrocyte
$K_{\mathbf{f,g,ldh}}$	9.0365	$mM^{-1}s^{-1}$	Forward rate constant for LDH in the astrocyte
$K_{\mathbf{r,g,ldh}}$	8.286×10^{-1}	$mM^{-1}s^{-1}$	Reverse rate constant for LDH in the astrocyte
$V_{\mathbf{max,g,mito}}$	8.906×10^{-3}	mM/s	Forward rate constant for LDH in the astrocyte
$V_{\mathbf{max,ge,LAC}}$	2.678×10^{-1}	mM/s	Maximum reaction rate for the mitochondrial response for the astrocyte
$K_{\mathbf{m,ge,LAC}}$	3.816×10^{-1}	mM	Reaction rate constant for LAC exchange between astrocytes and ECS
$V_{\mathbf{max,gc,LAC}}$	7.0974×10^{-5}	mM/s	Maximum rate for LAC exchange between astrocytes and capillary
$K_{\mathbf{m,gc,LAC}}$	3.731×10^{-6}	mM	Reaction constant for LAC exchange between astrocytes and capillary
$V_{\mathbf{max,g,ATPase}}$	3.0484×10^{-2}	mM/s	Maximum rate of ATP consumption for cellular processes in the astrocyte
$k_{\mathbf{r,g,ck}}$	4.806×10^{-1}	$mM^{-1}s^{-1}$	Reverse reaction rate constant for CK in the astrocyte
$k_{\mathbf{f,g,ck}}$	6.236×10^{-1}	$mM^{-1}s^{-1}$	Forward reaction rate constant for CK in the astrocyte
$PScap_g$	1.147×10^{-1}	s^{-1}	O^2 mass transfer constant between capillary and astrocytes
$K_{m,\mathbf{ce,GLC}}$	6.831	mM	Reaction constant for GLC exchange between the capillary and the ECS
$V_{\mathbf{m,ce,GLC}}$	4.508×10^{-2}	mM/s	Reaction rate for GLC exchange between the capillary and the ECS
$K_{\mathbf{m,ec,LAC}}$	2.094×10^{-2}	mM	Reaction constant for LAC exchange between the capillary and the ECS
$V_{\mathbf{m,ec,LAC}}$	1.324×10^{-1}	mM/s	Reaction rate for LAC exchange between the capillary and the ECS
$V_{\mathbf{max,g,gs}}$	5.230×10^{-3}	mM/s	Maximum exchange rate for GLU exchange between the neuron and astrocyte
$V_{\mathbf{max,eg,GLU}}$	1.518×10^{-2}	mM/s	Maximum rate for GLU exchange between the ECS and the astrocyte
$V_{\mathbf{max,gys}}$	2.919×10^{-5}	mM/s	Maximum rate for GLY synthase at the astrocyte

$K_{m,gys}$	1.536×10^{-5}	mM	Rate constant for GLY synthase at the astrocyte
$V_{max,glyp}$	2.856×10^{-5}	mM/s	Maximum rate for GLY phosphorylase at the astrocyte
$K_{m,GLY}$	$.690\times10^{-4}$	mM	Rate for GLY phosphorylase at the astrocyte
$K_{m,PYR}$	1.171×10^{-2}	mM	Affinity constant of mitochondria for PYR
$K_{m,ATP}$	2.049×10^{-3}	mM	Affinity constant of mitochondria for ATP
$K_{i,ATP}$	7.894×10^{-1}	mM	Affinity constant of PFK for ATP
$K_{m,ADP}$	3.186×10^{-8}	mM	Affinity constant of ADP
$K_{m,O2}$	6.182×10^{-4}	mM	Affinity constant of O_2
$K_{m,GLC}$	1.680×10^{-1}	mM	Affinity constant of GLC
$K_{m,GLU}$	6.767×10^{-2}	mM	Affinity constant of GLC
$K_{m,G6P}$	5.322×10^{-1}	mM	Affinity constant of G6P
$K_{m,F6P,pgi}$	7.120×10^{-2}	mM	Affinity constant of PGI for F6P
$K_{m,F6P,pfk}$	1.887×10^{-1}	mM	Affinity constant of PGI for PFK
$K_{m,pump}$	4.264×10^{-1}	mM	Affinity constant of ATP for NaK-pump
K_{O_2}	4.895×10^{-2}	mM	O_2 transport constant
q_{ak}	3.427×10^{-1}	dimentionless	Equilibrium constant for AK
nH	3.492	dimentionless	Hill coefficient for ATP inhibition
$K_{m,hk,ATP}$	1.094×10^{-3}	mM	Michaelis-Menten rate of ATP for HK
$K_{m,pfk,ATP}$	7.104×10^{-6}	mM	Michaelis-Menten rate of ATP for PFK

B. Fitting water co-transporters to the ionic model

In order to add the ionic channels permeable to water as described in Østby et al. (2009) the model of cellular ionic movement by Orlowski et al. (2013) had to be adapted. This resulted in the following kinetics.:

$$\frac{d[Na]_g}{dt} = \frac{-iNa_g - iNaK_g - iNaCa_g + iNKCC - 3\times iGTR1_g}{VF} - \gamma_g.[Na]_g \quad \text{(B1)}$$

$$\frac{d[Na]_n}{dt} = \frac{-iNa_n - iNaK_n - iNaCa_n - 3\times iGTR1_n}{VF} - \gamma_n.[Na]_n \quad \text{(B2)}$$

$$\frac{d[K]_g}{dt} = \frac{iK_g + iNaK_g + iNKCC + iGTR1_g}{VF} - \gamma_g.[K]_g \quad \text{(B3)}$$

$$\frac{d[K]_n}{dt} = \frac{iK_n + iNaK_n + iGTR1_n}{VF} - \gamma_n.[K]_n \quad \text{(B4)}$$

$$\frac{d[Ca]_g}{dt} = \frac{iCa_g + iNaCa_g}{VF} - \gamma_g.[Ca]_g \quad \text{(B5)}$$

$$\frac{d[Ca]_n}{dt} = \frac{iCa_n + iNaCa_n}{VF} - \gamma_n.[Ca]_n \quad \text{(B6)}$$

$$\frac{d[Cl]_g}{dt} = \frac{iCl_g - 2\times iNKCC}{VF} - \gamma_g.[Cl]_g \quad \text{(B7)}$$

$$\frac{d[Cl]_n}{dt} = \frac{iCl_n}{V\times F} - \gamma_n.[Cl]_n \quad \text{(B8)}$$

$$\frac{d[GLU]_g}{dt} = \frac{-iGLU_g + iGTR1_g}{VF} - \gamma_g.[GLU]_g \quad \text{(B9)}$$

$$\frac{d[GLU]_n}{dt} = \frac{-iGLU_n + iGTR1_n}{VF} - \gamma_n.[GLU]_n \quad \text{(B10)}$$

where, the currents iNa_c, iK_c, iCl_c, iCa_c are the currents through the ion specific channels for sodium, potassium, chloride and calcium respectively; $iNaK_c$ stands for the sodium potassium pump; $iNaCa_c$ is the sodium-calcium co-transporter and γ_g and γ_n are the rate of change to the concentration of the ion due to volume change.

Before refitting the model further alteration to the Orlowski et al. (2013) model were required due to the implementation of glutamate Nernst potential. This is because the potential depends on the quotient between the intra and extra cellular glutamate concentrations. Orlowski et al. (2013) assumes that both the astrocyte and the ECS have no glutamate at steady state, which would result on indeterminate Nernst potential. To overcome this limitation of the model the concentrations of glutamate for the astrocyte and ECS were replaced with the concentrations in Dronne et al. (2006).

These new concentrations of glutamate alter the osmotic pressure in these compartments. Therefore the model required recalibration. The steps presented in Section 2.1 in the work by Orlowski et al. (2013) were followed:

1. The concentration of chloride at the ECS is calculated to ensure the compartment is electrically neutral which means:
$$[Na^+]_e + [K^+]_e + 2 \times [Ca^{2+}]_e - [HCO_3^-]_e - [Cl^-]_e - [GLU^-]_e = 0 \quad \text{(B11)}$$
2. The intracellular concentration of chloride is calculated to make the Nernst potential equal to -70 mV.
3. Then it is assumed that there are impermeable anions (A_i) inside the cell that ensure that the net osmotic pressure across the membrane is zero:
$$([Na^+]_i + [K^+]_i + [Ca^{2+}]_i + [HCO_3^-]_i + [Cl^-]_i + [GLU^-]_i + [A^-]_i) - ([Na^+]_e + [K^+]_e + [Ca^{2+}]_e + [HCO_3^-]_e + [Cl^-]_e + [GLU^-]_e) = 0 \quad \text{(B12)}$$
4. Finally, the A_i charge (z_{A_i}) is calculated to ensure the intra-cellular space is neutrally charged; which means:
$$[Na^+]_i + [K^+]_i + 2 \times [Ca^{2+}]_i - [HCO_3^-]_i - [Cl^-]_i - [GLU^-]_i - z_{A_i}[A^-]_i = 0 \quad \text{(B13)}$$

In the following Table B1 all the initial conditions found in the literature and the ones calculated are presented.

Table B1: Initial conditions and parameters for the ionic model.

Parameter	Value	Units	Reference
$[\boldsymbol{Na^+}]_{n,g}$	19	mM	Orlowski et al. (2013)
$[\boldsymbol{Na^+}]_e$	140	mM	Orlowski et al. (2013)
$[\boldsymbol{K^+}]_{n,g}$	5	mM	Orlowski et al. (2013)
$[\boldsymbol{K^+}]_e$	130	mM	Orlowski et al. (2013)
$[\boldsymbol{Ca^{2+}}]_{n,g}$	0.0006	mM	Orlowski et al. (2013)
$[\boldsymbol{Ca^{2+}}]_e$	2.0023	mM	Orlowski et al. (2013)
$[\boldsymbol{Cl^-}]_{n,g}$	9.0360	mM	Calculated
$[\boldsymbol{Cl^-}]_e$	124.0036	mM	Calculated
$[\boldsymbol{HCO_3^-}]_{n,g}$	15.77	mM	Orlowski et al. (2013)
$[\boldsymbol{HCO_3^-}]_e$	25	mM	Orlowski et al. (2013))
$[\boldsymbol{GLU^-}]_{n,g}$	3	mM	Dronne et al. (2006)
$[\boldsymbol{GLU^-}]_e$	0.001	mM	Dronne et al. (2006)
$[\boldsymbol{A^-}]_{n,g}$	119.2003	mM	Calculated
$\boldsymbol{z_{A_{n,g}}}$	1.0168	dimensionless	Calculated

With these new ionic concentrations the permeability of the channels in Orlowski et al. (2013) model and the new channels are fitted to ensure the ionic currents are stable at steady state. The resulting permeabilities can be seen in Table B2.

Table B2: Fitted ionic channel permeabilities.

Parameter	Value	Units	Description
kK_n	168140	pA	Permeability of the of the neuronal potassium channel.
kNa_n	29104.3	pA	Permeability of the sodium channel at the neuron.
kCa_n	810.679	pA	Calcium channel permeability at the neuron.
kCl_n	2532.07	pA	Chloride channel permeability at the neuron.
$kNaK_n$	41.1898	pA	Sodium potassium pump permeability for the neuron.
$kNaCa_n$	49.3498	pA	Sodium calcium co-transporter neuronal permeability
$kGTR1_n$	4.76×10^{-5}	pS/μm^2	Neuronal glutamate transporter permeability.
$kGLU_n$	3.36×10^{-5}	pS/μm^2	Glutamate channels permeability at the neuron.
kNa_g	164871	pA	The glial sodium channel permeability
kK_g	164871	pA	Potassium channel permeability at the astrocyte.
kCa_g	819.409	pA	Glial calcium channel permeability.
kCl_g	2319.28	pA	Permeability of the glial chloride channel.
$kNaK_g$	39.9515	pA	Glial sodium and potassium pump permeability
$kNaCa_g$	50.0884	pA	Calcium and sodium glial co-transporter permeability
$kNKCC_g$	1.68×10^{-5}	pS/μm^2	Sodium-potassium and chloride glial permeability
$kGTR1_g$	4.65×10^{-5}	pS/μm^2	Glial glutamate transporter permeability
$kGLU_g$	3.28×10^{-5}	pS/μm^2	Glutamate glial channel permeability

C. Parameters and kinetics of the new volume model

Adding all the components described in Section 3.1 the astrocytic, neuronal and ECS volume kinetics can be summarized in Equations C1 – C3 respectively:

$$\frac{dV_g}{dt} = M\frac{iNKCC + iGTR1_g}{VF} + \frac{S_g M}{RTV}\left[(k_0 + \gamma k_{aqp})[\Delta H_{cg} - \Delta\pi_{cg}] - (k_0 + (1-\gamma)k_{aqp})[\Delta H_{ge} - \Delta\pi_{ge}]\right] \quad \text{(C1)}$$

$$\frac{dV_n}{dt} = M\frac{iGTR1_n}{VF} + \frac{S_n M}{RTV}k_n[\Delta H_{ne} - \Delta\pi_{ne}] \quad \text{(C2)}$$

$$\frac{dV_e}{dt} = -\frac{dV_n}{dt} - M\frac{iNKCC + iGTR1_g}{VF} - MV_w + \frac{S_g M}{RTV}(k_0 + (100-n)k_{aqp})[\Delta H_{ge} - \Delta\pi_{ge}] + k_c[\Delta H_{ce} - \Delta\pi_{ce}] - V_{gli} \quad \text{(C3)}$$

The volume of the capillary is assumed to stay constant throughout the simulations.
The list of initial conditions and constants can be found in Table C1.

Table C1: Initial conditions and parameters of the compartmental volume kinetics.

	Value	Units	Description	Reference
Initial conditions				
V_g	0.25	dimensionless	Volume fraction of astrocyte	Orlowski et al. (2013)
V_n	0.45	dimensionless	Volume fraction of the neuron	Orlowski et al. (2013)
V_{ECS}	0.20	dimensionless	Volume fraction of the ECS	Orlowski et al. (2013)
Parameters and constants				
H_g	12.3930	kPa	Net intra-glial hydrostatic pressure	calculated
H_n	-4.99	kPa	Net intra-neuronal hydrostatic pressure	Kimelberg (2004)
H_{ECS}	-5	kPa	Net Hydrostatic pressure at the ECS	Kimelberg (2004)
H_c	15	kPa	Capillary net hydrostatic pressure	Kimelberg (2004)
π_c	762.9104	kPa	Net osmotic pressure at the capillary	Solenov et al. (2004)
V_v	-2.88	/s	Rate of fluid extraction from the ECS by the ventricles	calculated
k_0	7×10^{-5}	m/s	Astrocytic membrane permeability not due to AQP4	Solenov et al. (2004)
k_{aqp}	4.3×10^{-4}	m/s	Astrocytic membrane permeability due to AQP4	Solenov et al. (2004)
k_n	3×10^{-4}	m/s	Neuronal membrane permeability	Steriade and McCarley (2013)
k_c	3.2×10^{-15}	$m^3/(kPa.s)$	Capillary rate of plasma filtration	Fenstermacher and Johnson (1966)
M	1.807×10^{-7}	L/mmole	Water molar volume at 310.15 K	Cohen (2008)
V	25,000	μm^3	Total volume of space considered	Dronne et al. (2006)
S_g	2,092.41	μm^2	Astrocitic surface area	Dronne et al. (2006)
S_n	2,244.66	μm^2	Neuronal surface area	Dronne et al. (2006)
F	96,485.309	C/mole	Faraday constant	Orlowski et al. (2013)
R	8,309.97904	mVC/(molK)	Gas constant	Orlowski et al. (2013)
T	310.15	K	Temperature	Orlowski et al. (2013)

D. Complement model

The work by Korotaevskiy et al. (2009) has extensively researched the literature for measurements of protein concentrations and kinetics. The later was defined based on the work by Morgan and Harris (1999) where the molar mass (kDa) and concentration (mg/dm^3) of the inactive complement proteins were measured in human plasma. From these the concentration in mM/dm^3 was calculated as:

$$\frac{mmole}{dm^3} = \frac{g/dm^3}{kDa} \quad \text{(D1)}$$

The full list of concentrations can be seen in Table D1.

Table D1: Concentration of complement proteins

Protein	Molecular mass (kDa)	Concentration (mg/dm^3)	Concentration (mM/dm^3)
$\boldsymbol{C_1}$	620	180	1.16×10^{-4}
$\boldsymbol{C_2}$	102	20	8×10^{-5}
$\boldsymbol{C_3}$	185	1300	2.8×10^{-3}
$\boldsymbol{C_4}$	205	600	1.16×10^{-3}
$\boldsymbol{C_5}$	190	70	1.48×10^{-4}
$\boldsymbol{C_6}$	120	65	2.16×10^{-4}
$\boldsymbol{C_7}$	110	55	2×10^{-4}
$\boldsymbol{C_8}$	152	55	1.44×10^{-4}
$\boldsymbol{C_9}$	69	60	3.6×10^{-4}

Additionally, the work by Korotaevskiy et al. (2009) was able to compile the concentration of inhibitory proteins present in the inactive state from the literature, as seen table D2.

Table D2: Concentration of complement inhibitors

Protein	Molecular mass (kDa)	Concentration (mg/dm^3)	Concentration (mM/dm^3)
$\boldsymbol{C_{1inh}}$	104	177	6.8×10^{-4}
$\boldsymbol{C_{4bp}}$	468	248	2.12×10^{-4}
$\boldsymbol{S}$	70	315	1.8×10^{-3}
$\boldsymbol{Clusterin}$	80	70	3.48×10^{-4}

The remaining intermediate proteins were assumed to have concentration 0 mM at the start of the simulations. The kinetics of the whole complement model by Korotaevskiy et al. (2009)defined as:

$$\frac{d([C_1])}{d(t)} = -\left(K^p_{c1est}\right)[C_1]\,[C_{AQP4-NMO}] \quad \text{(D2)}$$

$$\frac{d([C_{1est}])}{d(t)} = K^p_{c1est}C1\ ([C_{AQP4-NMO}] - [C_{1est}]) - K^p_{C1est-C1inh}\ [C_{1est}]\,[C_{1inh}] \quad \text{(D3)}$$

$$\frac{d([C_4])}{d(t)} = -\frac{K^{C1est}_{catC4}\,[C_4][C_{1est}]}{K^{C1est}_{mC4}\left(1 + \frac{[C_4]}{K^{C1est}_{mC4}} + \frac{[C_{4b2}]}{K^{C1est}_{mC4b2}}\right)} \quad \text{(D4)}$$

$$\frac{d([C_{4b}])}{d(t)} = \frac{K_{catC4}^{C1est}\,[C_4]\,[C_{1est}]}{K_{mC4}^{C1est}\left(1 + \frac{[C_4]}{K_{mC4}^{C1est}} + \frac{[C_{4b2}]}{K_{mC4b2}^{C1est}}\right)} - K_{c4b2}^{p}\,[C_{4b}]\,[C_2] + K_{C4b2}^{n}\,[C_{4b2}] + K_{c4b2a}^{n}\,[C_{4b2a}] - K_{c4b,c4bp}^{p}\,[C_{4b}]\,[C_{4bp}] + K_{c4b,c4bp}^{n}\,[C_{4b,4bp}] \quad \text{(D5)}$$

$$\frac{d([C_2])}{d(t)} = -K_{c4b2}^{p}\,[C_{4b}]\,[C_2] + K_{C4b2}^{n}\,[C_{4b2}] \quad \text{(D6)}$$

$$\frac{d([C_{4b2}])}{d(t)} = K_{c4b2}^{p}\,[C_{4b}]\,[C_2] - K_{C4b2}^{n}\,[C_{4b2}] - \frac{K_{catC4b2}^{C1est}\,[C_{4b2}]\,[C_{1est}]}{K_{mC4b2}^{C1est}\left(1 + \frac{[C_4]}{K_{mC4}^{C1est}} + \frac{[C_{4b2}]}{K_{mC4b2}^{C1est}}\right)} \quad \text{(D7)}$$

$$\frac{d([C_3])}{d(t)} = -\frac{K_{catc3}^{c4b2a}\,[C_3]\,[C_{4b2a}]}{K_{mC3}^{C4b2a} + [C_3]} \quad \text{(D8)}$$

$$\frac{d([C_{3b}])}{d(t)} = \frac{K_{catc3}^{c4b2a}\,[C_3]\,[C_{4b2a}]}{K_{mC3}^{C4b2a} + [C_3]} - K_{C4b2a3b}^{p}\,[C_{4b2a}]\,[C_{3b}] + K_{C4b2a3b}^{n}\,[C_{4b2a3b}] \quad \text{(D9)}$$

$$\frac{d([C_{3a}])}{d(t)} = \frac{K_{catc3}^{c4b2a}\,[C_3]\,[C_{4b2a}]}{K_{mC3}^{C4b2a} + [C_3]} \quad \text{(D10)}$$

$$\frac{d([C_{4b2a}])}{d(t)} = \frac{K_{catC4b2}^{C1est}\,[C_{4b2}]\,[C_{1est}]}{K_{mC4b2}^{C1est}\left(1 + \frac{[C_4]}{K_{mC4}^{C1est}} + \frac{[C_{4b2}]}{K_{mC4b2}^{C1est}}\right)} - K_{C4b2a}^{n}\,[C_{4b2a}] - K_{C4b2a3b}^{p}\,[C_{4b2a}]\,[C_{3b}] + K_{C4b2a3b}^{n}\,[C_{4b2a3b}] \quad \text{(D11)}$$

$$\frac{d([C_{4b2a3b}])}{d(t)} = K_{C4b2a3b}^{p}\,[C_{4b2a}]\,[C_{3b}] - K_{C4b2a3b}^{n}\,[C_{4b2a3b}] \quad \text{(D12)}$$

$$\frac{d([C_5])}{d(t)} = -\frac{K_{catC5}^{C4b2a3b}\,[C_5]\,[C_{4b2a3b}]}{K_{mC5}^{C4b2a3b} + [C_5]} \quad \text{(D13)}$$

$$\frac{d([C_{5a}])}{d(t)} = \frac{K_{catC5}^{C4b2a3b}\,[C_5]\,[C_{4b2a3b}]}{K_{mC5}^{C4b2a3b} + [C_5]} \quad \text{(D14)}$$

$$\frac{d([C_{5b}])}{d(t)} = \frac{K_{catC5}^{C4b2a3b}\,[C_5]\,[C_{4b2a3b}]}{K_{mC5}^{C4b2a3b} + [C_5]} - K_{c5b6}^{p}\,[C_{5b}]\,[C_6] + K_{c5b6}^{n}\,[C_{5b6}] \quad \text{(D15)}$$

$$\frac{d([C_6])}{d(t)} = -K_{c5b6}^{p}\,[C_{5b}][C_6] + K_{c5b6}^{n}\,[C_{5b6}] \quad \text{(D16)}$$

$$\frac{d([C_7])}{d(t)} = -K_{c5b67}^{p}\,[C_{5b6}]\,[C_7] + K_{c5b67}^{n}\,[C_{5b67}] \quad \text{(D17)}$$

$$\frac{d([C_8])}{d(t)} = -K_{c5b678}^{p}\,[C_{5b67}][C_8] + K_{c5b678}^{n}\,[C_{5b678}] \quad \text{(D18)}$$

$$\frac{d([C_9])}{d(t)} = -K_{c5b6789}^{p}\,[C_{5b678}][C_9] + K_{c5b6789}^{n}\,[C_{5b6789}] \quad \text{(D19)}$$

$$\frac{d([C_{5b6}])}{d(t)} = K_{c5b6}^{p}\,[C_{5b}]\,[C_6] - K_{c5b6}^{n}\,[C_{5b6}] - K_{c5b67}^{p}\,[C_{5b6}][C_7] + K_{c5b67}^{n}\,[C_{5b67}] \quad \text{(D20)}$$

$$\frac{d([C_{5b67}])}{d(t)} = K_{c5b67}^{p}\,[C_{5b6}]\,[C_7] - K_{c5b67}^{n}\,[C_{5b67}] - K_{c5b678}^{p}\,[C_{5b67}]\,[C_8] + K_{c5b678}^{n}\,[C_{5b678}] - K_{c5b67s}^{p}\,[C_{5b67}]\,[S] + K_{c5b67s}^{n}\,[C_{5b67s}] \quad \text{(D21)}$$

$$\frac{d([C_{5b678}])}{d(t)} = K_{c5b67}^{p}\,[C_{5b67}]\,[C_8] - K_{c5b678}^{n}\,[C_{5b678}] - K_{c5b6789}^{p}\,[C_{5b678}]\,[C_9] + K_{c5b6789}^{n}\,[C_{5b6789}] - K_{c5b678Clu}^{p}\,[C_{5b678}]\,Clu] + K_{c5b678Clu}^{n}\,[C_{5b678Clu}] \quad \text{(D22)}$$

$$\frac{d([C_{5b6789}])}{d(t)} = K^{p}_{c5b6789}\ [C_{5b678}]\,[C_9] - K^{n}_{c5b6789}\ [C_{5b6789}] \quad \text{(D23)}$$

$$\frac{d([C_{1inh}])}{d(t)} = -K^{p}_{C1est-C1inh}\ [C_{1est}]\,[C_{1inh}] \quad \text{(D24)}$$

$$\frac{d([C_{4bp}])}{d(t)} = -K^{p}_{c4b,c4bp}\,[C_{4b}]\ [C_{4bp}] + K^{n}_{c4b,c4bp}[C_{4b,4bp}] \quad \text{(D25)}$$

$$\frac{d([C_{4b,4bp}])}{d(t)} = K^{p}_{c4b,c4bp}\,[C_{4b}]\ [C_{4bp}] - K^{n}_{c4b,c4bp}\,[C_{4b,4bp}] \quad \text{(D26)}$$

$$\frac{d([S])}{d(t)} = -K^{p}_{c5b67s}\ [C_{5b67}]\,[S] + K^{n}_{c5b67s}\ [C_{5b67s}] \quad \text{(D27)}$$

$$\frac{d([C_{5b67s}])}{d(t)} = K^{p}_{c5b67s}\,[C_{5b67}][S] - K^{n}_{c5b67s}\ [C_{5b67s}] \quad \text{(D28)}$$

$$\frac{d([Clu])}{d(t)} = -K^{p}_{c5b678Clu}\ [C_{5b678}]\,[Clu] + K^{n}_{c5b67Clu}\ [C_{5b678Clu}] \quad \text{(D29)}$$

$$\frac{d([C_{5b678Clu}])}{d(t)} = K^{p}_{c5b678Clu}\ [C_{5b678}]\,[Clu] - K^{n}_{c5b67Clu}\ [C_{5b678Clu}] \quad \text{(D30)}$$

The values of the different rates in Korotaevskiy et al. (2009) were found in the literature where possible and the remaining were fitted. In Table D3 all the values for the model are defined.

Table D3: Parameter values for the kinetics presented in the work by Korotaevskiy et al. (2009)

Parameter	Value	Units	Description
K^{p}_{C1est}	39.08	$mM^{-1}s^{-1}$	Formation of C_{1est}
$K^{p}_{C1est-C1inh}$	60	$mM^{-1}s^{-1}$	Dissociation rate of inhibitor C_{1inh} and C_{1est}
K^{C1est}_{catC4}	5	s^{-1}	Rate of C_4 activation by NMO-IgG and AQP4 binding
K^{C1est}_{mC4}	1×10^{-3}	mM	Rate of C_4 activation by NMO-IgG and AQP4 binding
K^{C1est}_{mC4b2}	1×10^{-4}	mM^{-1}	Rate of C_{4b2} activation by the NMO-IgG/AQP4/C_{1est} complex
K^{p}_{c4b2}	33.33	$mM^{-1}s^{-1}$	Rate of C_{4b2} formation
K^{n}_{C4b2}	33.33	s^{-1}	Rate of C_{4b2} dissociation
$K^{p}_{c4b,c4bp}$	200	$mM^{-1}s^{-1}$	Rate of $C_{4b2,4bp}$ formation
$K^{n}_{c4b,c4bp}$	1.6×10^{-2}	s^{-1}	Rate of $C_{4b2,4bp}$ dissociation
$K^{C1est}_{catC4b2}$	41.6	s^{-1}	Rate of C_{4b2} activation by the NMO-IgG/AQP4/C_{1est} complex
K^{c4b2a}_{catc3}	5.83	s^{-1}	Rate of C_3 activation by the C_{4b2a} complex
K^{C4b2a}_{mC3}	3×10^{-3}	mM	Rate of C_3 activation by the C_{4b2a} complex
$K^{p}_{C4b2a3b}$	1266.67	mM	Rate C_{4b2a3b} formation
$K^{n}_{C4b2a3b}$	4.67×10^{-3}	mM/s	Rate C_{4b2a3b} dissociation
$K^{C4b2a3b}_{catC5}$	2×10^{-2}	$mM^{-1}s^{-1}$	Rate of C_5 activation by the C_{4b2a3b} complex
$K^{C4b2a3b}_{mC5}$	5.1×10^{-6}	mM	Rate of C_5 activation by the C_{4b2a3b} complex
K^{p}_{c5b6}	60	$mM^{-1}s^{-1}$	Rate C_{5b6} formation
K^{n}_{c5b6}	0	s^{-1}	Rate C_{5b6} dissociation
K^{p}_{c5b67}	733.3	$mM^{-1}s^{-1}$	Rate C_{5b67} formation
K^{n}_{c5b67}	0	s^{-1}	Rate C_{5b67} dissociation

K^{p}_{c5b678}	1100	$mM^{-1}s^{-1}$	Rate C_{5b678} formation
K^{n}_{c5b678}	0	s^{-1}	Rate C_{5b678} dissociation
$K^{p}_{c5b6789}$	2833	$mM^{-1}s^{-1}$	Rate C_{5b6789} formation
$K^{n}_{c5b6789}$	0	s^{-1}	Rate C_{5b6789} dissociation
K^{p}_{c5b67s}	240	$mM^{-1}s^{-1}$	Rate C_{5b67s} formation
K^{n}_{c5b67s}	2.34	s^{-1}	Rate C_{5b67s} dissociation
$K^{p}_{c5b678Clu}$	416.7	$mM^{-1}s^{-1}$	Rate $C_{5b678Clu}$ formation
$K^{n}_{c5b678Clu}$	4×10^{-3}	s^{-1}	Rate $C_{5b678Clu}$ dissociation

E. Ion movement through lytic holes

In order to calculate the permeability k_C of the hole to each ion, two constants need to be calculated. Firstly there is the average number of channels n of a particular in a cellular membrane with surface area of 2,092.41 μm^2:

Table E1: Cellular membrane channel density.

Ions	Density [/um2]	Reference	n_P
Na+	5	Sontheimer et al. (1994)	10,462
Ca2+	0.5	Sherman et al. (1990)	1,046.2
K+	5000	Marom et al. (1996)	10,462,000
Cl-	62	Reisert et al. (2003)	129,729

Secondly the diameter of ratio r between the channels (r_P) and the holes ($r_h = 8\ nm$) using the Poiseuille's equation:

Table E2: Ionic channel radii.

Ions	Diameter r_P [A]	Reference	r_P
Na+	120	Sato et al. (1998).	1.234×10^{-2}
Ca2+	6.2	Perez,(2004)	1.732×10^{3}
K+	12	Jiang et al., (2002)	123.459259277778
Cl-	5	Wadiche et al., (1995)	4096

Then the permeability of each ion channel from Orlowski et al. (2013) (k_{0P}) can be adapted to take into consideration the parameters n_P and r_P as:

$$k_{h,P} = \frac{k_P}{n_P}\left(\frac{r_h}{r_P}\right)^2 \quad \text{(E1)}$$

Then the ionic channel equations presented in Orlowski et al. (2013)are adapted to include the formation of holes and the individual k_C.

Table E3: Kinetics of the ionic currents through the lytic holes.

Ions	Equation	
Na^+	$iNa = H.k_{Na}.sinh\left(\frac{v - vNa}{2.Vt}\right)$	(E2)
Ca^{2+}	$iCa = H.k_{ca}.sinh\left(\frac{v - vCa}{Vt}\right)$	(E3)

K^+	$iK = H.k_k . sinh\left(\frac{v - vK}{2.Vt}\right)$	(E4)
Cl^-	$iCl = H.k_{Cl}. sinh\left(\frac{v + vCl}{Vt}\right)$	(E5)

where v is the membrane potential; vCl, vK, vNa and vCa are the Nernst potentials of chloride, potassium, sodium and calcium respectively and $Vt = \frac{RT}{F}$, where R is the gas constant, T is temperature and F is the Faraday constant.

F. Model created to fit the CD59 data.

In order to create the CD59 inhibition model the experimental procedure fro (Saadoun et al., 2010) was mimicked. The aim of the work was to quantify the sensitivity of complement from different species to CD59. The procedure consists of injecting human complement into a culture of chicken erythrocytes. The proteins injected are C7, C8, C9 and protein complex C5b6. The work by Rollins et al. (1991) only mentions the mass of C7, C8 and C5b6. These need to be converted to mM by considering the molar mass values of the proteins in Korotaevskiy et al. (2009) and the volume presented in Rollins et al. (1991) of 1 mL. These conversions are shown in the table below. In the case of the proteins C8 and C9 they were taken from Korotaevskiy et al. (2009).

Table F1: Complement proteins concentration.

Protein	Mass [g]	Molar mass [Da]	Moles	Concentration [mM]	Reference
C5b6	2.70×10^{-7}	3.28×10^{5}	1.04×10^{10}	1.04×10^{-4}	Rollins et al. (1991)
C7	1.50×10^{-8}	1.10×10^{5}	3.64×10^{11}	3.64×10^{-5}	Rollins et al. (1991)
C8	(…)	1.52×10^{5}	(…)	3.6×10^{-4}	Korotaevskiy et al., (2009)
C9	(…)	6.90×10^{4}	(…)	9×10^{-4}	Korotaevskiy et al., (2009)

Then different concentrations of CD59 are injected into the medium where again the mass in g is presented and it has to be converted to concentration in mM. The molar mass was found to be 2×10^4 Da, also taken from Rollins et al. (1991).

Table F2: Calculation of CD59 concentration

Mass [g]	Moles	Concentration [mM]
5.00×10^{-08}	2.50×10^{-12}	2.50×10^{-6}
1.00×10^{-07}	5.00×10^{-12}	5.00×10^{-6}
1.50×10^{-07}	7.50×10^{-12}	7.50×10^{-6}
2.50×10^{-07}	1.25×10^{-11}	1.25×10^{-5}
5.00×10^{-07}	2.50×10^{-11}	2.50×10^{-5}
1.00×10^{-06}	5.00×10^{-11}	5.00×10^{-5}

The inhibition of MAC formation is measured by Rollins et al. (1991)by considering the percentage of lysis inhibited when compared to complement lysis when there is no CD59 present. The results in humans were extracted from Figure 5.1 from Rollins et al. (1991).

Table F3: Data taken from Rollins et al. (1991) of lysis inhibition by increasing concentrations of CD59.

CD59 [ug]	0	0.03	0.065	0.25	0.36	0.55	1
% Lysis	100	40	25	15	5	3	1

Then a mathematical model based on the work of Korotaevskiy et al. (2009) was created.

$$\frac{d([C7])}{d(t)} = -K_1[C5b6][C7] + K_2[C5b67] \quad \text{(F1)}$$

$$\frac{d([C8])}{d(t)} = -K_3[C5b67][C8] + K_4[C5b678] \quad \text{(F2)}$$

$$\frac{d([C9])}{d(t)} = -K_5[C5b678][C9] + K_6[C5b6789] \quad \text{(F3)}$$

$$\frac{d([C5b6])}{d(t)} = K_2[C5b67] - K_1[C5b6][C7] \quad \text{(F4)}$$

$$\frac{d([C5b67])}{d(t)} = K_1[C5b6][C7] - K_2[C5b67] - K_3[C5b67][C8] + K_4[C5b678] \quad \text{(F5)}$$

$$\frac{d([C5b678])}{d(t)} = K_3[C5b67][C8] - K_4[C5b678] - K_5[C5b678][C9] + K_6[C5b6789] - K_7[CD59][C5b678] + K_8[CD59Cb8] \quad \text{(F6)}$$

$$\frac{d([C5b6789])}{d(t)} = K_5[C5b678][C9] - K_6[C5b6789] - K_9[CD59][C5b6789] + K_{10}[CD59MAC] \quad \text{(F7)}$$

$$\frac{d([CD59])}{d(t)} = -K_7[CD59][C5b678] + K_8[CD59Cb8] - K_9[CD59][C5b6789] + K_{10}[CD59MAC] \quad \text{(F8)}$$

$$\frac{d([CD59Cb8])}{d(t)} = K_7[CD59][C5b678] - K_8[CD59Cb8] \quad \text{(F9)}$$

$$\frac{d([CD59MAC])}{d(t)} = K_9[CD59][C5b6789] - K_{10}[CD59MAC] \quad \text{(F10)}$$

The parameters are defined mostly as in Korotaevskiy et al. (2009)except for the ones fitted (K_7, K_8, K_9 and K_{10}). In the following Table the values for the parameters can be seen:

Table F4: Kinetics of the model created to fit to CD59 inhibition data.

Parameter	Value	Units	Reference	Parameter	Value	Units	Reference
$\boldsymbol{K_1}$	733.3	$mM^{-1}s^{-1}$	Korotaevskiy et al. (2009)	K_6	0	s^{-1}	Korotaevskiy et al. (2009)
$\boldsymbol{K_2}$	0	s^{-1}	Korotaevskiy et al. (2009))	K_7	0.0157	s^{-1}	Fitted

K_3	1100	$mM^{-1}s^{-1}$	Korotaevskiy et al. (2009))	K_8	0.001019	$mM^{-1}s^{-1}$	Fitted
K_4	0	s^{-1}	Korotaevskiy et al. (2009)	K_9	0.04337	s^{-1}	Fitted
K_5	2833.33	$mM^{-1}s^{-1}$	Korotaevskiy et al. (2009)	K_{10}	0.15011	$mM^{-1}s^{-1}$	Fitted

Appendix G: Adapted cytotoxic oedema model by Orlowski *et al.* (2013)

Table G.1: Variables of Cloutier model

Variable		Steady-state value	Differential equation
Extracellular states			
GLC_e	Glucose	0.47	$\frac{\partial GLC_e}{\partial t} = v_{GLC}^{ce} - \left(\left(v_{GLC}^{eg}\frac{1}{Reg}\right) + v_{GLC}^{en}\frac{1}{Ren}\right) - y_e GLC_e$
LAC_e	Lactate	0.37	$\frac{\partial LAC_e}{\partial t} = v_{LAC}^{ne}\frac{1}{Ren} + v_{LAC}^{ge}\frac{1}{Reg} - v_{LAC}^{ec} - y_e LAC_e$
Astrocytic and neuronal states			
$O2_n$	Oxygen	0.102	$\frac{\partial O2_n}{\partial t} = R_{en}v_{LAC}^{ne} + R_{eg}v_{LAC}^{ge} - v_{LAC}^{ec} - y_n O2_n$
$O2_g$	Oxygen	0.102	$\frac{\partial O2_g}{\partial t} = R_{en}v_{LAC}^{ne} + R_{eg}v_{LAC}^{ge} - v_{LAC}^{ec} - y_g O2_g$
Capillary			
$O2_c$	Oxygen	7.46	$\frac{\partial O2_c}{\partial t} = v_{O2}^{c} - v_{O2}^{nc}\frac{1}{Rcn} + v_{O2}^{cg}\frac{1}{Rcg}$
$CO2_c$	Carbon dioxide	2.12	$\frac{\partial CO2_c}{\partial t} = kCO2(CO2_{c2} - CO2_c) - 2\frac{Fin_t}{V_c}(CO2_c - CO2_a)$
GLC_c	Glucose	4.6401	$\frac{\partial GLC_c}{\partial t} = v_{GLC}^{c} - \left(v_{GLC}^{ce}\frac{1}{Rce} + v_{GLC}^{cg}\frac{1}{Rcg}\right)$
LAC_c	Lactate	0.3251	$\frac{\partial LAC_c}{\partial t} = v_{LAC}^{c} + (v_{LAC}^{ec} \times (\frac{1}{Rce}) + v_{LAC}^{gc} \times (\frac{1}{Rcg}))$
Other states			
Vv	Venous volume	0.0237	$\frac{\partial Vv}{\partial t} = F_{int} - F_{out}$
F_{in}	Capillary entering blood flow		$F_{int} = CBF_0 + CBFc\ CBF0\left(\frac{1}{1+e^{-30(t-s)}} - \frac{1}{1+e^{-30(time-(s+d))}}\right)$

$\boldsymbol{F_{out}}$	Capillary leaving blood flow	$F_{out} = \frac{Fin\_t \times \left(\frac{Vv}{Vv0}\right)^{2} + tv \times \left(\frac{Vv}{Vv0}\right)^{-\frac{1}{2}} \times \frac{F_{int}}{Vv0}}{1 + F_{int} \times tv \times \left(\frac{Vv}{Vv0}\right)^{-\frac{1}{2}} \times \frac{1}{Vv0}}$

Table G.2: Kinetic equations for exchange and transport systems

No	Reaction	Differential equation
Transport		
1	GLC exchange between capillary and extracellular fluid	$v_{GLC}^{ce} = vmax_{GLC}^{ce}\left(\frac{GLCc}{GLCc + Km_{ce_{GLC}}} - \frac{GLCe}{GLCe + Km_{ce_{GLC}}}\right)$
2	GLC exchange between extracellular fluid and astrocytes	$v_{GLC}^{cg} = vmax_{GLC}^{cg}\left(\frac{GLCc}{GLCc + Km_{cg_{GLC}}} - \frac{GLCg}{GLCg + Km_{cg_{GLC}}}\right)$
3	GLC exchange between extracellular fluid and neurons	$v_{GLC}^{en} = vmax_{GLC}^{en}\left(\frac{GLCe}{GLCc + Km_{en_{GLC}}} - \frac{GLCn}{GLCn + Km_{en_{GLC}}}\right)$
4	GLC exchange between extracellular fluid and astrocytes	$v_{GLC}^{eg} = vmax_{GLC}^{eg}\left(\frac{GLCe}{GLCc + Km_{eg_{GLC}}} - \frac{GLCg}{GLCg + Km_{eg_{GLC}}}\right)$
5	LAC exchange between extracellular fluid and capillary	$v_{LAC}^{ec} = vmax_{LAC}^{ec}\left(\frac{LACe}{(LACe + Km_{ec_{LAC}})} - \frac{(LACc)}{(LACc + Km_{ec_{LAC}})}\right)$
6	LAC exchange between neurons and extracellular fluid	$v_{LAC}^{ne} = vmax_{LAC}^{ne}\left(\frac{LACn}{(LACn + Km_{ne_{LAC}})} - \frac{(LACe)}{(LACe + Km_{ne_{LAC}})}\right)$
7	LAC exchange between astrocytes and extracellular fluid	$v_{LAC}^{ge} = vmax_{LAC}^{ge}\left(\frac{LACg}{(LACg + Km_{ge_{LAC}})} - \frac{(LACe)}{(LACe + Km_{ge_{LAC}})}\right)$
8	LAC exchange between astrocytes and capillary	$v_{LAC}^{gc} = vmax_{LAC}^{gc}\left(\frac{LACg}{(LACg + Km_{ge_{LAC}})} - \frac{(LACc)}{(LACc + Km_{gc_{LAC}})}\right)$
9	O2 exchange between capillary and neurons	$v_{O2}^{cn} = \frac{PScapn}{Vn}\left(Ko2\ \left(\frac{HbOP}{O2c} - 10\right)^{-\frac{1.0}{nh_{O2}}} - O2n\right)$
10	O2 exchange between capillary and astrocytes	$v_{O2}^{cg} = \frac{PScapg}{Vg}\left(Ko2\ \left(\frac{HbOP}{O2c} - 1.0\right)^{-\frac{1.0}{nh_{O2}}} - O2g\right)$
11	Blood flow contribution to capillary O2	$vc_{O2} = 2\left(\frac{Fin_t}{Vc}\right)(O2a - O2c)$
12	Blood flow contribution to capillary GLC	$vc_{GLC} = 2\left(\frac{Fin_t}{Vc}\right)(GLCa - GLCc)$
13	Blood flow contribution to capillary LAC	$v_{LAC}^{c} = 2\left(\frac{Fin_t}{Vc}\right).(LACa - LACc)$

Table G.3: Central energy metabolism

Variable		Steady-state value	Differential equation
Neuronal states			
$\boldsymbol{GLC_n}$	Glucose	0.43	$\frac{\partial GLC_n}{\partial t} = v_{GLC}^{en} - v_{HK}^{n} - y_n GLC_n$
$\boldsymbol{G6P_n}$	Glucose-6-P	0.75	$\frac{\partial G6P_n}{\partial t} = v_{HK}^{n} - v_{PGI}^{n} - v_{C6PDH}^{n} - y_n G6P_n$

$\boldsymbol{F6Pn}$	Fructose-6-P	0.2	$\frac{\partial F6P_n}{\partial t} = v^n_{PGI} - v^n_{PFK} - v^n_{PPP} - y_n F6P_n$
$\boldsymbol{GAP_n}$	Glyceraldehyde-3-P	0.05	$\frac{\partial GAP_n}{\partial t} = 2.v^n_{PFK} - v^n_{PGK} - v^n_{mito} - y_n GAP_n$
$\boldsymbol{PEP_n}$	Phosphoenolpyruvate	0.025	$\frac{\partial PEP_n}{\partial t} = v^n_{PGK} - v^n_{PK} - y_n PEP_n$
$\boldsymbol{LAC_n}$	Lactate	0.28	$\frac{\partial LAC_n}{\partial t} = v^n_{LDH} - v^{en}_{LAC} - y_n LAC_n$
$\boldsymbol{ATP_n}$	Adenosine triphosphate	2.25	$\frac{\partial ATP_n}{\partial t} = \left[-v^n_{HK} - v^n_{PFK} + v^n_{PGK} + v^n_{PK} + 15v^n_{mito} + v^n_{CK} - v^n_{pump,Na} - v^n_{ATPase}\right]\left[1 - \frac{dAMP_n}{dATP_n}\right]^{-1} - y_n ATPn$
$\boldsymbol{NADH_n}$	Nicotinamide adenine dinucleotide reduced	0.04	$\frac{\partial NADH_n}{\partial t} = v^n_{PGK} - v^n_{LDH} - v^n_{mito} - y_n NADHn \; with \; NADH_n + NAD_n = NADH_{tot}$
$\boldsymbol{PCr_n}$	Phosphocreatine	4.6401	$\frac{\partial PCr_n}{\partial t} = -v^n_{CK} \; with \; PCr_n + Cr_n = PCr_{tot}$
Astrocyte states			
$\boldsymbol{GLC_g}$	Glucose	0.43	$\frac{\partial GLC_g}{\partial t} = v^{eg}_{GLC} - v^g_{HK} - y_g GLC_g$
$\boldsymbol{G6P_g}$	Glucose-6-P	0.75	$\frac{\partial G6P_g}{\partial t} = v^g_{HK} - v^g_{PGI} - v^g_{C6PDH} - y_g G6P_g$
$\boldsymbol{F6P_g}$	Fructose-6-P	0.2	$\frac{\partial F6P_g}{\partial t} = v^g_{PGI} - v^g_{PFK} - v^g_{PPP} - y_g F6P_g$
$\boldsymbol{GAP_g}$	Glyceraldehyde-3-P	0.05	$\frac{\partial GAP_g}{\partial t} = 2v^g_{PFK} - v^g_{PGK} - v^g_{mito} - y_g GAP_g$
$\boldsymbol{PEP_g}$	Phosphoenolpyruvate	0.025	$\frac{\partial PEP_g}{\partial t} = v^g_{PGK} - v^g_{PK} - y_g PEP_g$
$\boldsymbol{LAC_g}$	Lactate	0.28	$\frac{\partial LAC_g}{\partial t} = v^g_{LDH} - v^{eg}_{LAC} - y_g LAC_g$
$\boldsymbol{ATP_g}$	Adenosine triphosphate	2.25	$\frac{\partial ATP_g}{\partial t} = \left[-v^g_{HK} - v^g_{PFK} + v^g_{PGK} + v^g_{PK} + 15.v^g_{mito} + v^g_{CK} - v^g_{pump,Na} - v^g_{ATPase}\right]\left[1 - \frac{dAMP_g}{dATP_g}\right]^{-1}$
$\boldsymbol{NADH_g}$	Nicotinamide adenine dinucleotide reduced	0.04	$\frac{\partial NADH_g}{\partial t} = v^g_{PGK} - v^g_{LDH} - v^g_{mito} \; with \; NADH_g + NAD_g = NADH_{tot}$
$\boldsymbol{PCr_g}$	Phosphocreatine	4.6401	$\frac{\partial PCr_g}{\partial t} = -v^g_{CK} \; with \; PCr_g + Cr_g = PCr_{tot}$

Table G.4: Kinetic equations for central energy metabolism

No.	Reaction	Differential equation
Neuronal metabolism		
1	Hexokinase	$v^n_{HK} = vmax^n_{HK}\left[\frac{ATP_n}{ATP_n + Km_{hk_{ATP}}}\right]\left[\frac{GLCn}{GLCn + Km_{ce_{GLC}}}\right][1 - f(G6P_n, 0.6, 20)]$
2	Phosphoglucose isomerase	$v^n_{PGI} = vmax^n_{f,PGI}\left[\frac{G6Pn}{G6Pn + Km_{G6P}}\right] - vmax^n_{f,F6P}\left[\frac{F6Pn}{F6Pn + Km_{F6P-PGI}}\right]$
3	Phosphofructokinase	$v^n_{PFK} = k^n_{PFK}\left[\frac{ATP_n}{ATP_n + Km_{PFk_{ATP}}}\right]\left[1 + \left(\frac{ATP_n}{KI_{ATP}}\right)^{nH}\right]^{-1}\left[\frac{F6Pn}{F6Pn + Km_{F6P-PFK}}\right]$

4	Phosphoglycerate kinase	$v_{PGK}^{n} = k_{PGK}^{n} GAPnADPn \left[\frac{NADn}{NADHn}\right]$
5	Pyruvate Kinase	$v_{PK}^{n} = k_{PK}^{n} PEPnADPn$
6	Mitochondrial oxidation of pyruvate	$v_{mito}^{n} = v_{max,mito}^{n} \left[\frac{PYRn}{PYRn + Km_{PYR}}\right]\left[\frac{ADPn}{ADPn + Km_{ADP}}\right] \left[\frac{O2n}{O2n + Km_{O2n}}\right]\left[\frac{NADn}{NADn + Km_{NAD}}\right]\left[\frac{NADHn}{NADHn + Km_{NADH}}\right] \left[1 - f(\frac{ATPn}{ADPn}, 20,5)\right]$
7	Lactate dehydrogenase	$v_{LDH}^{n} = k_{LDH,f}^{n} PYR_n NADH_n - k_{LDH,f}^{n} LAC_n NAD_n$
8	Creatine kinase	$v_{CK}^{n} = k_{CK,f}^{n} PCr_n ADP_n - k_{CK,r}^{n} Cr_n ATP_n$
9	ATPase (excluding Na-ATPase)	$v_{ATPase}^{n} = V_{max,ATPase}^{n} \left[\frac{ATP_n}{ATP_n + K_{m,ATP}}\right]$
Astrocyte metabolism		
10	Hexokinase	$v_{HK}^{g} = k_{HK}^{g} . \left[\frac{ATP_g}{ATP_g + Km_{hk_{ATP}}}\right]\left[\frac{GLCg}{GLCg + Km_{ce_{GLC}}}\right] [1 - f(G6P_g, 0.6,20)]$
11	Phosphoglucose isomerase	$v_{PGI}^{g} = vmax_{f,PGI}^{g} \left[\frac{G6Pg}{G6Pg + Km_{G6P}}\right] - vmax_{f,F6P}^{g} \left[\frac{F6Pg}{F6Pg + Km_{F6P}}\right]$
12	Phosphofructokinase	$v_{PFK}^{g} = k_{PFK}^{g} \left[\frac{ATP_n}{ATP_n + Km_{PFk_{ATP}}}\right]\left[1 + \left(\frac{ATP_g}{KI_{ATP}}\right)^{gH}\right]^{-1} \left[\frac{F6Pg}{F6Pg + Km_{F6P}}\right]$
13	Phosphoglycerate kinase	$v_{PGK}^{g} = k_{PGK}^{g} GAPgADPg \left[\frac{NADg}{NADHg}\right]$
14	Pyruvate Kinase	$v_{PK}^{g} = k_{PK}^{g} PEPgADPg$
15	Mitochondrial oxidation of pyruvate	$v_{mito}^{g} = v_{max,mito}^{g} \left[\frac{PYRg}{PYRg + Km_{PYR}}\right]\left[\frac{ADPg}{ADPg + Km_{ADP}}\right] \left[\frac{O2g}{O2g + Km_{O2n}}\right]\left[\frac{NADg}{NADg + Km_{NAD}}\right]\left[\frac{NADHg}{NADHg + Km_{NADH}}\right] \left[1 - f(\frac{ATPg}{ADPg}, 20,5)\right]$
16	Lactate dehydrogenase	$v_{LDH}^{g} = v_{LDH,f}^{g} PYR_g NADH_g - v_{LDH,f}^{g} LAC_g NAD_g$
17	Creatine kinase	$v_{CK}^{g} = k_{CK,f}^{g} PCr_g ADP_g - k_{CK,r}^{g} Cr_g ATP_g$
18	ATPase (excluding Na-ATPase)	$v_{ATPase}^{g} = V_{max,ATPase}^{g} \left[\frac{ATP_g}{ATP_g + K_{m,ATP}}\right]$

Adenylate kinase (AK) equilibrium (neurons and astrocytes)

$$ADP = \frac{ATP}{2}\left[-q_{AK} + \sqrt{u}\right]$$

$$\frac{dAMP}{dATP} = -1 + \frac{q_{AK}}{2} - 0.5.\sqrt{u} + q_{AK}\frac{ANP}{ATP\sqrt{u}} \qquad \text{with } u = q_{AK}^2 + 4q_{AK}\left(\frac{ANP}{ATP} - 1\right)$$

Table G.5: Glycogen storage system

No.	Reaction	Differential equation
Astrocytic state		
$\boldsymbol{GLY_g}$	Glycogen	$\frac{\partial GLY_g}{\partial t} = v_{GLYS}^{g} - v_{GLYP}^{g}$
Kinetic equations		
1	Glycogen synthase	$v_{GLYS}^{g} = v_{max,GLYS}^{g} \left[\frac{G6Pg}{G6Pg + Km_{G6P}}\right]$
2	Glycogen phosphorylase	$v_{GLYP}^{g} = v_{max,GLYP}^{g} \left[\frac{G6Pg}{G6Pg + Km_{G6P}}\right]\frac{GLYg}{GLY0}$
3	GLY regulation	$f_{GLY} = \Delta_{GLY}\left[f\left(t, t_{0,GLY}, 4\right) - f\left(t, t_{0,GLY} + t_{end,GLY}, 4\right)\right]^{*}$

Table G.6: Physical constants and known concentrations

Parameter name	Value	Description	Units
$\boldsymbol{NADH_{tot}}$	0.22	Total NAD+NADH	mM
$\boldsymbol{PCr_{tot}}$	5.0	Total $PCr + Cr$	mM
$\boldsymbol{O_{2a}}$	8.34	Arterial O_2 concentration	mM
$\boldsymbol{CO_{2a}}$	1.2	Arterial CO_2 concentration	mM
$\boldsymbol{GLC_a}$	4.8	Arterial GLC concentration	mM
$\boldsymbol{LAC_a}$	0.313	Arterial LAC concentration	mM
$\boldsymbol{k_{pump}}$	3.17×10^{-7}	Transport rate constant	cm.mM.s^{-1}
$\boldsymbol{CBF_0}$	0.012	Cerebral blood flow steady state value	s^{-1}
$\boldsymbol{nOP}$	15	Oxidative phosphorylation ratio	dimensionless
$\boldsymbol{V_{V,0}}$	0.0236	Base venous volume	dimensionless
$\boldsymbol{HbOP}$	8.6	O_2 concentration with haemoglobin	mM
$\boldsymbol{F}$	96500	Molecular charge	C.mol^{-1}
$\boldsymbol{RT}$	2577340	Perfect gas constant and temperature	kPa
$\boldsymbol{V_m}$	-70	Membrane potential	mV
$\boldsymbol{GLY_0}$	2.5	Steady state value of GLY	mM

Table G.7: States of the ionic species involved in the pH model

Variable		Steady-state value	Differential equation
Neuronal states			
$\boldsymbol{H_n}$	Hydrogen ions	3.98×10^{-5}	$\frac{\partial H_n}{\partial t} = v^n_{buffer} - v^n_{CK} - \frac{\partial ATP_n}{\partial t} + \frac{\partial LAC_n}{\partial t} + v^n_{NHE} - y_n H_n$
$\boldsymbol{HCO3_n}$	Bicarbonate	15.77	$\frac{\partial HCO3_n}{\partial t} = k_{f2}\, H2CO3_n + k_{b3} CO3_{2n}\, H_n - k_{f3} HCO3_n - k_{b2} H_n HCO3_n - y_n HCO3_n$
$\boldsymbol{CO3_{2n}}$	Carbon trioxide	0.01989	$\frac{\partial CO3_{2n}}{\partial t} = k_{f3}\, HCO3_n - k_{b3} CO3_{2n}\, H_n - y_n CO3_{2n}$
$\boldsymbol{H2CO3_n}$	Carbonic acid	0.0015	$\frac{\partial H2CO3_n}{\partial t} = k_{f1} CO3_{c2} + k_{b2}\, HCO3_n H_n - (k_{f2} + k_{b1}) H2CO3_n - y_n H2CO3_n$

Astrocyte states			
$\boldsymbol{H_g}$	Hydrogen ions	3.98×10^{-5}	$\frac{\partial H_g}{\partial t} = v^g_{buffer} - v^g_{CK} - \frac{\partial ATP_g}{\partial t} + \frac{\partial LAC_g}{\partial t} + v^g_{NHE} - y_g H_g$
$\boldsymbol{HCO3_g}$	Bicarbonate	15.77	$\frac{\partial HCO3_g}{\partial t} = k_{f2}\, H2CO3_g + k_{b3} CO3_{2g}\, H_g - k_{f3} HCO3_g - k_{b2} H_g HCO3_g - y_g HCO3_g$
$\boldsymbol{CO3_{2g}}$	Carbon trioxide	0.01989	$\frac{\partial CO3_{2g}}{\partial t} = k_{f3}\, HCO3_g - k_{b3} CO3_{2g}\, H_g - y_g CO3_{2g}$
$\boldsymbol{H2CO3_g}$	Carbonic acid	0.0015	$\frac{\partial H2CO3_g}{\partial t} = k_{f1} CO3_{c2} + k_{b2}\, HCO3_g H_g - (k_{f2} + k_{b1}) H2CO3_g - y_g H2CO3_g$
ECS states			
$\boldsymbol{H_e}$	Hydrogen ions	0.0000631	$\frac{\partial H_e}{\partial t} = v^e_{buffer} + \frac{1}{R_{eg}}\frac{\partial LAC_g}{\partial t} + \frac{1}{R_{en}}\frac{\partial LAC_n}{\partial t} + \frac{1}{R_{eg}} v^g_{NHE} + \frac{1}{R_{en}} v^n_{NHE} - y_e H_e$
$\boldsymbol{HCO3_e}$	Bicarbonate	25	$\frac{\partial HCO3_g}{\partial t} = k_{f2}\, H2CO3_e + k_{b3} CO3_{2e}\, H_e - k_{f3} HCO3_e - k_{b2} H_e HCO3_e - y_e HCO3_e$
$\boldsymbol{CO3_{2e}}$	Carbon trioxide	0.05	$\frac{\partial CO3_{2e}}{\partial t} = k_{f3}\, HCO3_e - k_{b3} CO3_{2e}\, H_e - y_e CO3_{2e}$
$\boldsymbol{H2CO3_e}$	Carbonic acid	0.0015	$\frac{\partial H2CO3_e}{\partial t} = k_{f1} CO3_{c2} + k_{b2}\, HCO3_e H_e - (k_{f2} + k_{b1}) H2CO3_e - y_n H2CO3_e$
Capillary states			
$\boldsymbol{CO2_{c2}}$	Carbon dioxide	2.5	$\frac{\partial CO2_{c2}}{\partial t} = \frac{\left(\frac{1}{Rcn} v^n_{c_{CO2}} + \frac{1}{Rcg} v^g_{c_{CO2}} - k_{CO2}\,(CO2_{c2} - CO2_c)\right)}{\left(\frac{1 - V_c}{V_c}\right)}$

Table G.8: Kinetic equations for the pH model

No.	Reaction	Differential equation
Neuron		
1	Cellular buffer solution	$v^n_{buffer} = k_{f3} HCO3_n - k_{b3} CO3_{2n} H_n - k_{b2} HCO3_n H_n + k_{f2}\, H2CO3_n$
2	Na^+/H^+ antiporter	$v^n_{NHE} = \begin{cases} \frac{-v^{Na}_{max}(Na_e - Na_n)}{VF(K^{Na}_m + Na_e - Na_n)} \frac{1}{1 + e^{\alpha(-6.7 + pH_n)}} 1000 & when\ \ pH \le 7.2 \\ 0 & otherwise \end{cases}$
3	pH calculation from H^+ concentration	$pH_n = -\log\left(\frac{H_n}{1000}\right)$
Astrocyte		
4	Cellular buffer solution	$v^g_{buffer} = k_{f3} HCO3_g - k_{b3} CO3_{2g} H_g - k_{b2} HCO3_g H_g + k_{f2}\, H2CO3_g$
5	Na^+/H^+ antiporter	$v^g_{NHE} = \begin{cases} \frac{-v^{Na}_{max}(Na_e - Na_g)}{VF(K^{Na}_m + Na_e - Na_g)} \frac{1}{1 + e^{\alpha(-6.7 + pH_g)}} 1000 & when\ \ pH \le 7.2 \\ 0 & otherwise \end{cases}$
6	pH calculation from H^+ concentration	$pH_g = -\log\left(\frac{H_g}{1000}\right)$

Table G.9: Physical constants and known concentrations		
Parameter name	Value	Units
k_{f1}	0.11	s^{-1}
k_{f2}	1×10^{4}	s^{-1}
k_{f3}	1.03×10^{4}	s^{-1}
k_{b1}	183.33	s^{-1}
k_{b2}	9508.7	$M\ s^{-1}$
k_{b3}	8.1616×10^{10}	$M\ s^{-1}$
K_m^{Na}	23	mM
v_{max}^{Na}	10	pA

References

Cloutier, M., Bolger, F.B., Lowry, J.P., Wellstead, P., 2009. An integrative dynamic model of brain energy metabolism using in vivo neurochemical measurements. J. Comput. Neurosci. 27, 391–414.

Cohen, E.R., 2008. Quantities, units and symbols in physical chemistry. Royal Society of Chemistry, Cambridge, UK.

Dronne, M.-A., Boissel, J.-P., Grenier, E., 2006. A mathematical model of ion movements in grey matter during a stroke. J. Theor. Biol. 240, 599–615.

Fenstermacher, J., Johnson, J., 1966. Filtration and reflection coefficients of the rabbit blood-brain barrier. Am. J. Physiol. Content 211, 341–346.

Jiang, Y., Lee, A., Chen, J., Cadene, M., Chait, B.T., MacKinnon, R., 2002. The open pore conformation of potassium channels. Nature 417, 523–526.

Kimelberg, H., 2004. Water homeostasis in the brain: basic concepts. Neuroscience 129, 851–860.

Korotaevskiy, A.A., Hanin, L.G., Khanin, M.A., 2009. Non-linear dynamics of the complement system activation. Math. Biosci. 222, 127–143.

Marom, S., Salman, H., Lyakhov, V., Braun, E., 1996. Effects of density and gating of delayed-rectifier potassium channels on resting membrane potential and its fluctuations. J. Membr. Biol. 154, 267–274.

Morgan, B.P., Harris, A.L., 1999. Complement Regulatory Proteins. Academic Press.

Orlowski, P., O'Neill, D., Grau, V., Ventikos, Y., Payne, S., 2013. Modelling of the physiological response of the brain to ischaemic stroke. Interface Focus 3, 20120079.

Østby, I., Øyehaug, L., Einevoll, G.T., Nagelhus, E.A., Plahte, E., Zeuthen, T., Lloyd, C.M.,

Ottersen, O.P., Omholt, S.W., 2009. Astrocytic mechanisms explaining neural-activity-induced shrinkage of extraneuronal space. PLoS Comput Biol 5, e1000272.

Perez, K.T., 2004. Structure-function Relationship & Modulation Of The T-type Calcium Channel 1g. Leuven University Press, Leuven, Belgium.

Reisert, J., Bauer, P.J., Yau, K.-W., Frings, S., 2003. The Ca-activated Cl channel and its control in rat olfactory receptor neurons. J. Gen. Physiol. 122, 349–364.

Rollins, S.A., Zhao, J., Ninomiya, H., Sims, P.J., 1991. Inhibition of homologous complement by CD59 is mediated by a species-selective recognition conferred through binding to C8 within C5b-8 or C9 within C5b-9. J. Immunol. Baltim. Md 1950 146, 2345–2351.

Saadoun, S., Waters, P., Bell, B.A., Vincent, A., Verkman, A., Papadopoulos, M.C., 2010. Intra-cerebral injection of neuromyelitis optica immunoglobulin G and human complement produces neuromyelitis optica lesions in mice. Brain 133, 349–361.

Saltelli A, Tarantola S, Campolongo F, Ratto M., 2004. Sensitivity analysis in practice: a guide to assessing scientific models. Ispra, Italy: John Wiley & Sons

Sato, C., Sato, M., Iwasaki, A., Doi, T., Engel, A., 1998. The sodium channel has four domains surrounding a central pore. J. Struct. Biol. 121, 314–325.

Schmidt, H., Jirstrand, M., 2006. Systems Biology Toolbox for MATLAB: a computational platform for research in systems biology. Bioinformatics 22, 514–515.

Sherman, A., Keizer, J., Rinzel, J., 1990. Domain model for Ca2 (+)-inactivation of Ca2+ channels at low channel density. Biophys. J. 58, 985.

Solenov, E., Watanabe, H., Manley, G.T., Verkman, A., 2004. Sevenfold-reduced osmotic water permeability in primary astrocyte cultures from AQP-4-deficient mice, measured by a fluorescence quenching method. Am. J. Physiol.-Cell Physiol. 286, C426–C432.

Sontheimer, H., Fernandez-Marques, E., Ullrich, N., Pappas, C., Waxman, S., 1994. Astrocyte Na+ channels are required for maintenance of Na+/K (+)-ATPase activity. J. Neurosci. 14, 2464–2475.

Steriade, M.M., McCarley, R.W., 2013. Brainstem control of wakefulness and sleep. Springer Science & Business Media, New York, USA.

Wadiche, J.I., Amara, S.G., Kavanaugh, M.P., 1995. Ion fluxes associated with excitatory amino acid transport. Neuron 15, 721–728. doi:10.1016/0896-6273(95)90159-0